# FREE-SURFACE BOUNDARY LAYER AND THE ORIGIN OF BOW VORTICES



by

V. C. Patel, L. Landweber, and C. J. Tang

Sponsored by

Office of Naval Research
Special Focus Research Program in Ship Hydrodynamics
Contract No. N00014-83-K-0136

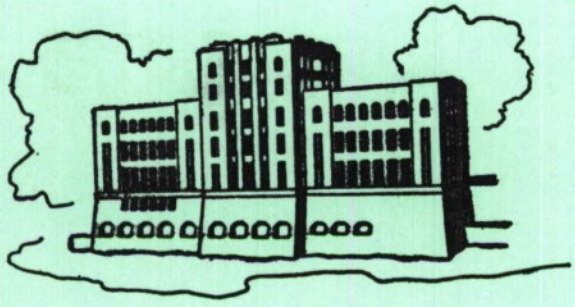

IIHR Report No. 284

Iowa Institute of Hydraulic Research
The University of Iowa
Iowa City, Iowa 52242



October 1984

# FREE-SURFACE BOUNDARY LAYER AND THE ORIGIN OF BOW VORTICES

by

V. C. Patel, L. Landweber, and C. J. Tang

Sponsored by

Office of Naval Research
Special Focus Research Program in Ship Hydrodynamics
Contract No. N00014-83-K-0136

IIHR Report No. 284

Iowa Institute of Hydraulic Research
The University of Iowa
Iowa City, Iowa 52242

October 1984

UNCLASSIFIED

SECURITY CLASSIFICATION OF THIS PAGE *(When Date Entered)*

| REPORT DOCUMENTATION PAGE | | READ INSTRUCTIONS BEFORE COMPLETING FORM |
|---|---|---|
| 1. REPORT NUMBER | 2. GOVT ACCESSION NO. | 3. RECIPIENT'S CATALOG NUMBER |
| 4. TITLE *(and Subtitle)*<br>Free-Surface Boundary Layer and the Origin of Bow Vortices | | 5. TYPE OF REPORT & PERIOD COVERED<br>Technical Report<br>Jan 1983-Sept 1984<br>6. PERFORMING ORG. REPORT NUMBER<br>IIHR Report No. 284 |
| 7. AUTHOR(s)<br>V.C. Patel, L. Landweber, C.J. Tang | | 8. CONTRACT OR GRANT NUMBER(s)<br>N00014-83-k-0136 |
| 9. PERFORMING ORGANIZATION NAME AND ADDRESS<br>Iowa Institute of Hydraulic Research<br>The University of Iowa<br>Iowa City, Iowa 52242 | | 10. PROGRAM ELEMENT, PROJECT, TASK AREA & WORK UNIT NUMBERS<br>NR 655-002 |
| 11. CONTROLLING OFFICE NAME AND ADDRESS<br>Office of Naval Research<br>800 North Quincy Street<br>Arlington, Virginia 22217 | | 12. REPORT DATE<br>October 1984<br>13. NUMBER OF PAGES<br>22 |
| 14. MONITORING AGENCY NAME & ADDRESS*(if different from Controlling Office)*<br>Office of Naval Research<br>536 South Clark Street<br>Chicago, Illinois 60605 | | 15. SECURITY CLASS. *(of this report)*<br>Unclassified<br>15a. DECLASSIFICATION/DOWNGRADING SCHEDULE |

16. DISTRIBUTION STATEMENT *(of this Report)*

Approved for Public Release; Distribution Unlimited

17. DISTRIBUTION STATEMENT *(of the abstract entered in Block 20, if different from Report)*

18. SUPPLEMENTARY NOTES

19. KEY WORDS *(Continue on reverse side if necessary and identify by block number)*

Free Surface Boundary Layer
Surface tension
Bow Vortices

20. ABSTRACT *(Continue on reverse side if necessary and identify by block number)*

The boundary layer that exists due to the boundary conditions at a curved free surface of a viscous liquid ahead of a body in motion is analyzed. It is shown that surface tension and viscous effects are important and together explain the occurrence of vortices which have been observed on ship bows. The equations of the free-surface boundary layer have been derived and an integral method has been suggested for their solution.

DD FORM 1 JAN 73 1473 EDITION OF 1 NOV 65 IS OBSOLETE

UNCLASSIFIED

SECURITY CLASSIFICATION OF THIS PAGE *(When Date Entered)*

# FREE-SURFACE BOUNDARY LAYER AND THE ORIGIN OF BOW VORTICES

## I. INTRODUCTION

The requirements of vanishing tangential stresses at a curved free surface imply a nonzero vorticity which is convected and diffused into the fluid. At sufficiently high Reynolds numbers, the vorticity is confined to a thin boundary layer along the free surface. The oscillatory boundary layer at the free surface of travelling and stationary water waves has been considered by Longuet-Higgins (1953, 1960), particularly to determine its effect on the mass-transport velocity in the fluid outside the boundary layer. Batchelor (1967) has also described the origin of the free-surface boundary layer and presented two applications, namely the drag of a spherical gas bubble rising through a liquid and the attenuation of gravity waves due to viscous effects at the free surface. A free-surface boundary layer is also present ahead of an object in motion due to the surface elevation above the undisturbed level and the associated curvature.

The possible importance of the free-surface boundary layer ahead of a body moving at the surface of a liquid, e.g., at the bow of a ship, was pointed out by Landweber and Patel (1979). A number of flow-visualization experiments have shown the existence of vortices under the free surface at the bow. Such vortices were first reported by Suzuki (1975) and Honji (1976) in two-dimensional flow ahead of a semi-submerged circular cylinder. Kayo et al. (1982) have repeated these experiments and confirmed the occurrence of these vortices. In three-dimensional flow, the experiments of Kayo and Takekuma (1981) and Shahshahan (1982) with towed ship models, those of Kayo et al. (1982) with towed vertical cylinders, and some ongoing observations made by the present authors with fixed cylinders in a hydraulic flume show horseshoe vortices forming ahead of the bow just below the free surface. Although bow vortices are also discussed in several recent papers (see Maruo, 1983; Mori, 1984; Takekuma and Eggers, 1984), the precise mechanism responsible for their formation, and the role they play in the breaking of bow waves, is not yet understood.

The two-dimensional free-surface boundary layer is the subject of the present paper. The necessary conditions at a curved free surface of a viscous fluid in motion are examined and it is shown that surface tension plays a critical role in determining the real flow ahead of an obstacle. In particular, the boundary conditions and the equation of continuity lead to a criterion for the occurrence of a stagnation point at the free surface, which may be identified with the existence of a vortex further downstream. The theory is in approximate agreement with the experimental observations in two-dimensional flow noted above, and may explain the origin of the bow vortices.

The equations of the free-surface boundary layer are then derived and an approximate integral method of solution is presented. This leads to an estimate of the momentum thickness of the boundary layer.

## II. NAVIER-STOKES EQUATIONS AND BOUNDARY CONDITIONS

Consider a two-dimensional obstacle in a uniform stream of velocity $U_\infty$, as shown in figure 1. The vertical distance above the undisturbed level far upstream is denoted by y and the elevation of the free surface above this level is $\zeta$. It is convenient to choose a curvilinear orthogonal coordinate system (s,n) in which s is along the free surface and n is normal to it. If the corresponding velocity components are denoted by u and v, then for laminar flow, the equation of continuity and the Navier-Stokes equations in the (s,n) directions may be written, respectively,

$$\frac{1}{h_1}\frac{\partial u}{\partial s} + \frac{\partial v}{\partial n} + \kappa_{12} v = 0 \tag{1}$$

$$\begin{aligned}\frac{u}{h_1}\frac{\partial u}{\partial s} + v\frac{\partial u}{\partial n} + \kappa_{12}uv + \frac{1}{h_1}\frac{\partial}{\partial s}\left(\frac{p}{\rho}\right) + \frac{g}{h_1}\frac{\partial y}{\partial s} \\ - \nu\left\{\frac{1}{h_1^2}\frac{\partial^2 u}{\partial s^2} + \frac{\partial^2 u}{\partial n^2} - \frac{1}{h_1^3}\frac{\partial h_1}{\partial s}\frac{\partial u}{\partial s} + \kappa_{12}\frac{\partial u}{\partial n}\right. \\ \left. + 2\kappa_{12}\frac{1}{h_1}\frac{\partial v}{\partial s} - \kappa_{12}^2 u + \frac{1}{h_1}\frac{\partial \kappa_{12}}{\partial s} v\right\} = 0\end{aligned} \tag{2}$$

$$\frac{u}{h_1}\frac{\partial v}{\partial s} + v\frac{\partial v}{\partial n} - \kappa_{12}u^2 + \frac{\partial}{\partial n}\left(\frac{p}{\rho}\right) + g\frac{\partial y}{\partial n}$$
$$- \nu\left\{\frac{1}{h_1^2}\frac{\partial^2 v}{\partial s^2} + \frac{\partial^2 v}{\partial n^2} - \frac{1}{h_1^3}\frac{\partial h_1}{\partial s}\frac{\partial v}{\partial s} + \kappa_{12}\frac{\partial v}{\partial n}\right.$$
$$\left. - 2\kappa_{12}\frac{1}{h_1}\frac{\partial u}{\partial s} - \frac{1}{h_1}\frac{\partial \kappa_{12}}{\partial s}u - \kappa_{12}^2 v\right\} = 0 \qquad (3)$$

where $\rho$ is density, $\nu$ is kinematic viscosity, $g$ is acceleration due to gravity, $p$ is pressure,

$$h_1 = 1 + \kappa n \qquad (4)$$

$$\kappa_{12} \equiv \frac{1}{h_1}\frac{\partial h_1}{\partial n} = \frac{\kappa}{1 + \kappa n} \qquad (5)$$

and $\kappa$ is the curvature of the free surface.

The normal and tangential stresses in the fluid, $\tau_{nn}$ and $\tau_{sn}$, respectively, are

$$\tau_{nn} = - p + 2\mu\frac{\partial v}{\partial n} \qquad (6)$$

$$\tau_{sn} = \mu\left\{h_1\frac{\partial}{\partial n}\left(\frac{u}{h_1}\right) + \frac{1}{h_1}\frac{\partial v}{\partial s}\right\} \qquad (7)$$

where $\mu$ $(= \rho\nu)$ is the coefficient of viscosity. The only component of vorticity is

$$\omega = \frac{1}{h_1}\left\{\frac{\partial v}{\partial s} - \frac{\partial}{\partial n}(h_1 u)\right\} \qquad (8)$$

At the free surface, we have

$$v_o = 0 \qquad (9)$$

and since the tangential stress vanishes, equation (7) gives

$$\left(\frac{\partial u}{\partial n}\right)_o = \kappa u_o \qquad (10)$$

where the subscript o denotes conditions at the free surface. Using equations (9) and (10) in equation (8), we obtain the expression for the vorticity at the free surface,

$$\omega_o = - 2 \kappa u_o \tag{11}$$

Thus, if the flow in the interior of the fluid is assumed to be irrotational, there exists a boundary layer across which the vorticity reduces to zero. Note that such a boundary layer is absent if the free surface is flat.

If surface tension is neglected, the normal stresses at the free surface must be constant and equal to the ambient pressure, which may be taken to be zero. Equation (6) then yields

$$\left(\frac{\partial v}{\partial n}\right)_o = 0$$

If this and equation (9) are used in the continuity equation (1), we obtain the rather surprising result

$$\left(\frac{\partial u}{\partial s}\right)_o = 0$$

i.e. $u_o$ = constant = $U_\infty$

Since the velocity at the free surface in inviscid flow decreases and vanishes at the intersection with the obstacle, or equivalently, since the velocity outside the boundary layer, $u_\delta$ say, must decrease as the obstacle is approached, the above result is physically unrealistic and we conclude that the condition of zero or constant normal stress at the free surface cannot be satisfied. In other words, the influence of surface tension cannot be ignored.

Denoting the surface tension by $\sigma$, the balance of normal stress across the free surface requires that

$$- p_a + \sigma\kappa = - p_o + 2 \mu \left( \frac{\partial v}{\partial n}\right)_o \tag{12}$$

where $p_a$ is the (zero) ambient pressure above the free surface and $p_o$ is the pressure in the liquid just at the free surface. Thus,

$$\left(\frac{\partial v}{\partial n}\right)_o = \frac{\kappa\,\sigma}{2\,\mu} - \frac{(p_a - p_o)}{2\,\mu} \tag{13}$$

Substitution of equations (9) and (13) into the continuity equation (1) now yields

$$\left(\frac{\partial u}{\partial s}\right)_o = -\frac{\kappa\,\sigma}{2\,\mu} + \frac{(p_a - p_o)}{2\,\mu} = -\frac{\sigma}{2\,\mu}\frac{d}{ds}(\arctan \zeta_x) + \frac{(p_a - p_o)}{2\,\mu} \tag{14}$$

where $\zeta_x = \frac{d\zeta}{dx}$ is the slope of the free surface. If, as a first approximation, we assume that $p_o = p_a$, i.e. the surface tension is balanced by the viscous stresses rather than a jump in pressure, equation (14) can be integrated to obtain

$$u_o = U_\infty - \frac{\sigma}{2\mu} \arctan \zeta_x \tag{15}$$

The distribution of vorticity at the free surface is then given by equations (11) and (15) as

$$\omega_o = -2\kappa\, u_o = -2\kappa\,(U_\infty - \frac{\sigma}{2\,\mu} \arctan \zeta_x) \tag{16}$$

Equation (15) shows that the velocity along the free surface decreases as $\zeta_x$ increases. The previous result of constant velocity in the absence of surface tension is recovered when $\sigma = 0$. It is quite surprising that, with the above approximation, the velocity and vorticity at the free surface can be predicted solely from kinematics (equations 1 and 9) and the stress conditions (equations 10 and 12) at the surface without recourse to the dynamical equations (2) and (3). Even more surprising is the fact that equation (15) embodies a SEPARATION CRITERION for the free-surface boundary layer, since $u_o = 0$ indicates a stagnation point on the free surface. Thus, for separation

$$\zeta_{x_{sep}} = \tan\left(\frac{2\mu U_\infty}{\sigma}\right)$$

$$= \tan\left(\frac{2W}{Re}\right) \tag{17}$$

where $\mathbf{W} = \frac{\rho U_\infty^2 L}{\sigma}$ and $\mathbf{Re} = \frac{\rho U_\infty L}{\mu}$ are the Weber and Reynolds numbers, respectively, based on some characteristic length L. Since $\zeta$ and $\zeta_x$ depend upon the Froude number, $\mathbf{F} = U_\infty / \sqrt{gL}$ say, equation (17) represents a separation criterion in terms of the three basic nondimensional parameters: **W**, **Re** and **F**.

## III. SEPARATION AT THE FREE SURFACE AND BOW VORTICES

In order to determine if equation (17) indeed represents a plausible result, we seek experimental confirmation. Consider the two-dimensional flow ahead of a semi-submerged circular cylinder of radius a with its axis horizontal and perpendicular to a stream of velocity $U_\infty$ in the positive x-direction, as shown in figure 2. Alternatively, the cylinder moves with velocity $U_\infty$ in the negative x-direction in a liquid at rest. The latter corresponds to the arrangement in the experiments of Suzuki (1975), Honji (1976) and Kayo et al. (1982). As mentioned in the Introduction, a vortex system was observed ahead of the cylinder as depicted in figure 2. Tests with different velocities indicated a wide variation in the length $\beta a$ of the vortex. However, the three sets of data appear to be in some conflict with regard to the influence of the cylinder speed on the length of the vortex. Although Suzuki appears to be first to observe the vortices, his measurements are related to the breaking of bow waves ahead of the cylinder rather than the size of the bow vortex. They are therefore not suitable for comparison with the present theory. The measurements of Honji, which are reproduced in figure 3, show an increase in $\beta$ with increasing Reynolds and Froude numbers. On the other hand, the observations of Kayo et al., shown in figure 4, indicate very large and scattered values of $\beta$ at the lowest velocities in the tests. With increasing velocity, $\beta$ appears to reach a minimum and show a moderate increase thereafter. Honji also showed that the size of the vortex decreased when the surface tension was reduced by adding detergents to the water. Similar observations were also made by Kayo et al. but no quantitative information was obtained for the case of the horizontal cylinder considered here.

If we identify the most upstream point S of the vortex (figure 2) with the free-surface stagnation point predicted by the present theory, then it is possible to calculate the distance $\beta a$ from equation (17), provided the slope

of the free surface $\zeta_x$ is known, or assumed, ahead of the cylinder. The determination of the free-surface elevation is of course the classical problem of nonlinear ship-wave theory.

### III.1 Evaluation of $\zeta_x$ from inviscid, irrotational-flow theory

Consider a circular cylinder of radius a, half immersed in a uniform stream of velocity $U_\infty$ in the positive direction of the x axis. Take the origin at the undisturbed water surface and the y-axis positive upwards. The irrotational-flow velocity components in the x- and y-directions are U and V, respectively, and the free-surface elevation due to the presence of the cylinder is $y = \zeta(x)$.

The condition that the free surface is a streamline gives

$$\zeta_x = V/U \tag{18}$$

while the Bernoulli equation for steady, irrotational flow and the zero-pressure condition at the free surface yields the implicit equation

$$f(x,y) = U^2 + V^2 + 2gy - U_\infty^2 = 0$$

The kinematic boundary condition, $Df/Dt = 0$, then yields the exact, nonlinear boundary condition

$$U(UU_x + VV_x) + V(UU_y + VV_y + g) = 0 \tag{19}$$

where the subscripts x, y denote derivatives. From the Cauchy-Riemann equations

$$U_x = -V_y, \qquad U_y = V_x \tag{20}$$

equation (19) becomes

$$V^2U_x - V(2UU_y + g) - U^2U_x = 0$$

which can be rewritten in the nondimensional form

$$V^2U_x - V(2UU_y + 1/(2F^2)) - U^2U_x = 0 \tag{21}$$

where (U,V) and (x,y) are scaled with $U_\infty$ and a, respectively, and the Froude number **F** is defined by

$$\mathbf{F} = \frac{U_\infty}{\sqrt{2ga}} \tag{22}$$

Combining equations (18) and (21), we obtain

$$\zeta_x = \frac{-4\mathbf{F}^2UU_x}{[(1+4\mathbf{F}^2UU_y)^2 + (4\mathbf{F}^2UU_x)^2]^{1/2} + 1 + 4\mathbf{F}^2UU_y} \tag{23}$$

which represents the free-surface slope upstream of the cylinder. Since, however, the velocity field and its derivatives are difficult to determine, especially close to the body, their values from the double-body approximation, i.e.,

$$U = 1 - \frac{1}{x^2+y^2} + \frac{2y^2}{(x^2+y^2)^2}, \quad V = -\frac{2xy}{(x^2+y^2)^2} \tag{24}$$

evaluated at y = 0, are used. The reason for using the double-body solution rather than that from linear wave theory is that the former, which considers the effect of nonlinearity, gives a better approximation to the velocity field near the body. A graph of $\zeta_x$ as a function of x/a is given in figure 5 for several values of the Froude number.

Substitution of $\zeta_x$ from equation (23) with U, $U_x$ and $U_y$ at y = 0 from equation (24) into equation (17) gives

$$\frac{8\mathbf{F}^2[(1+\beta)^2 - 1]}{\{(1+\beta)^{10} + 64\mathbf{F}^4[(1+\beta)^2 - 1]\} + (1+\beta)^5} = \tan\frac{2\mathbf{W}}{\mathbf{Re}} \tag{25}$$

which can be solved numerically (or graphically using figure 5) for the location of the separation point $\beta a$ (defined in figure 2) for given values of **F**, **Re** and **W**. When the equation has several positive roots, the largest one is taken since separation, if present, would occur at the most upstream point.

### III.2 Comparison with experimental results

Equation (25) has been solved for the conditions in the experiments of Honji (a = 0.05 m) and Kayo et al. (a = 0.10m). For Honji's data, the value of $\mu$ (= $1.22 \times 10^{-3}$ Ns/m$^2$) was inferred from the quoted Reynolds numbers and velocities. For the data of Kayo et al., their quoted value of $0.913 \times 10^{-3}$ Ns/m$^2$ was used. In both cases, $\sigma$ is assumed to take the standard value of 0.073 N/m. The results are shown by the dotted lines in figures 3 and 4. Note that, in both figures, the Reynolds and Froude numbers have been redefined consistently on the basis of the cylinder diameter, and the scales adjusted accordingly.

The results for Honji's experiments, which were conducted at very low Reynolds and Froude numbers, indicate qualitative agreement between theory and observations, but the predicted delayed separation indicates smaller vortices. In the case of Kayo et al., the theory predicts the trends at the higher Reynolds and Froude numbers but the calculations now indicate earlier separation and larger vortices. The experimental results at very low Froude numbers show considerable scatter. At the lowest Froude number in these tests, the experiments indicated very large separation distances which varied from test to test over a wide range. The authors noted that the largest distances were observed during the first experiment in the morning! The theory obviously does not predict this phenomenon.

In summary, we note that the present simple theory appears to provide an explanation for the origin of the bow vortices. The contradictions in the available experimental data indicate a need for more refined and controlled experiments. On the other hand, the disagreement between the theory and existing data could be due to a number of factors which need to explored further. Among these are (a) the influence of the assumption of no pressure jump across the free surface, (b) the uncertainty in the determination of the free-surface slope $\zeta_x$, (c) the interaction between the bow vortex and the shape of the free surface, (d) the occurrence of turbulent flow ahead of separation, and (e) the influence of surface contaminants in the experiments.

## IV. FREE-SURFACE BOUNDARY-LAYER EQUATIONS

The results presented above have been obtained solely from an examination of the boundary conditions at the free surface and the assumption that there is no pressure jump across the free surface. In order to remove the latter restriction it is necessary to seek a solution of the equations of motion.

The Navier-Stokes equations may be simplified to obtain the equations of the free-surface boundary layer. For this purpose, it is necessary to make an order-of-magnitude analysis utilizing the known boundary conditions. Let L be a characteristic length and $\delta$ be the boundary-layer thickness. Then $K^* \equiv \kappa L$, the nondimensional free-surface curvature which gives rise to the boundary layer, is controlled by the body geometry and the Froude number.

The equation of continuity (1) and its derivative are

$$\frac{\partial u}{\partial s} + h_1 \frac{\partial v}{\partial n} + \kappa v = 0 \tag{26}$$

$$\frac{\partial^2 u}{\partial s \partial n} + h_1 \frac{\partial^2 v}{\partial n^2} + 2\kappa \frac{\partial v}{\partial n} = 0 \tag{27}$$

Since $h_1 = O(1)$, from the former, we have

$$\frac{\partial v}{\partial n} = O\left(\frac{\partial u}{\partial s}\right) = O(1) \frac{U_\infty}{L} \tag{28}$$

and then

$$v = O\left(\frac{\delta}{L}\right) U_\infty \tag{29}$$

Also, equation (10) shows that

$$\frac{\partial u}{\partial n} = O(K^*) \frac{U_\infty}{L} \tag{30}$$

which gives

$$\frac{\partial^2 u}{\partial n^2} = O\left(\frac{K^* L}{\delta}\right) \frac{U_\infty}{L^2} \tag{31}$$

From equations (27) and (30), we obtain

$$\frac{\partial^2 v}{\partial n^2} = O(K^*) \frac{U_\infty}{L^2} \tag{32}$$

Now, since the first convective term, together with the pressure and gravity terms in the momentum equation (2), yields the Bernoulli equation, we conclude that the leading viscous term must be of order $(\kappa\delta)$, i.e.

$$\nu \frac{\partial^2 u}{\partial n^2} = O\left(\frac{K^* L}{Re\delta}\right) \frac{U_\infty^2}{L} = O(\kappa\delta) \frac{U_\infty^2}{L}$$

Hence

$$\frac{\delta}{L} = O\left(\frac{1}{\sqrt{Re}}\right) \tag{33}$$

and equations (29) and (31) become

$$v = O\left(\frac{1}{\sqrt{Re}}\right) U_\infty \tag{34}$$

$$\frac{\partial^2 u}{\partial n^2} = O\left(K^*\sqrt{Re}\right) \frac{U_\infty}{L^2} \tag{35}$$

Thus, we have the following results:

$$\begin{aligned} u &= O(1)\, U_\infty & v &= O\left(\frac{1}{\sqrt{Re}}\right) U_\infty \\ \frac{\partial u}{\partial n} &= O(K^*) \frac{U_\infty}{L} & \frac{\partial v}{\partial n} &= O(1) \frac{U_\infty}{L} \\ \frac{\partial^2 u}{\partial n^2} &= O\left(K^*\sqrt{Re}\right) \frac{U_\infty}{L^2} & \frac{\partial^2 v}{\partial n^2} &= O(K^*) \frac{U_\infty}{L^2} \end{aligned} \tag{36}$$

When the above orders of magnitude are introduced in the Navier-Stokes equations (1) - (3) and terms up to order $(\kappa\delta)$ are retained in each equation, we obtain the boundary-layer equations

$$\frac{\partial u}{\partial s} + \frac{\partial v}{\partial n} = 0 \tag{37}$$

$$u \frac{\partial u}{\partial s} + v \frac{\partial u}{\partial n} + \kappa u v + \frac{\partial}{\partial s}\left(\frac{p}{\rho} + gy\right) = \nu \frac{\partial^2 u}{\partial n^2} \tag{38}$$

$$-\kappa u^2 + \frac{\partial}{\partial n}\left(\frac{p}{\rho} + gy\right) = 0 \qquad (39)$$

## IV.1 Velocity Profile

The known boundary conditions can also be used to determine some characteristics of the velocity distribution across the boundary layer. To the first order, the vorticity, from equation (8), is

$$\omega \doteq -\frac{\partial u}{\partial n} - \kappa u \qquad (40)$$

The condition of zero vorticity outside the boundary layer yields

$$\left(\frac{\partial u}{\partial n}\right)_\delta \doteq -\kappa u_\delta \qquad (41)$$

For positive $\kappa$, equations (10) and (41) show that the velocity reaches a maximum within the boundary layer.

A velocity profile which explicitly satisfies the boundary conditions (10) and (41) is the cubic

$$u = u_o\left[1 + \kappa n + \frac{\kappa\alpha}{\delta} n^2 + \frac{\kappa\beta}{\delta^2} n^3\right] \qquad (42)$$

where

$$\beta = \frac{-(1+\alpha)(2+\kappa\delta)}{3+\kappa\delta} \doteq -\frac{2}{3}(1+\alpha) \qquad (43)$$

and $\alpha$ is a parameter which ensures compatibility with equation (2) at the free surface, i.e.

$$\alpha = \frac{\delta}{2\kappa u_o}\left(\frac{\partial^2 u}{\partial n^2}\right)_o = \frac{\delta}{2\nu\kappa u_o}\left(u_o u_o' + g\zeta' + \frac{p_o'}{\rho}\right)$$

where the primes denote derivatives with respect to s. The pressure $p_o$ can be eliminated from the above using the normal-stress condition (12) and the equation of continuity (37) since

$$p_o' = -\sigma\kappa' - 2\mu u_o'' \qquad (44)$$

Thus,

$$\alpha = \frac{\delta}{2\nu\kappa u_o} \left(u_o u_o' + g\zeta' - \frac{\sigma\kappa'}{\rho} - 2\nu u_o''\right) \tag{45}$$

It should be noted that the combination $(u_o u_o' + g\zeta')$ is small and therefore $\alpha$ is of order unity.

From equation (42), the ratio of velocity at the edge of boundary layer, $u_\delta$, to that at the free surface, $u_o$, can be expressed in terms of $\alpha$ as

$$\frac{u_\delta}{u_o} = \frac{3 + \kappa\delta(2+\alpha)}{3 + \kappa\delta} \doteq 1 + \frac{\kappa\delta}{3}(1+\alpha) \tag{46}$$

This indicates that $\alpha > -1$ for $u_\delta > u_o$.

## IV.2 Momentum Integral Equations

As a first step in the solution of the first-order boundary-layer equations (37)-(39), it is convenient to use the well-known integral method. Integration of the normal momentum equation (39) yields

$$\left(\frac{p}{\rho} + gy\right) = \left(\frac{p_o}{\rho} + g\zeta\right) + \int_o^n \kappa u^2 dn \tag{47}$$

and therefore

$$\left(\frac{p}{\rho} + gy\right)_\delta = \left(\frac{p_o}{\rho} + g\zeta\right) + \int_0^\delta \kappa u^2 dn \tag{48}$$

and

$$\frac{\partial}{\partial s}\left(\frac{p}{\rho} + gy\right) = \frac{d}{ds}\left(\frac{p_o}{\rho} + g\zeta\right) + \frac{\partial}{\partial s}\int_o^n \kappa u^2 dn \tag{49}$$

Now applying the Bernoulli equation at the edge of the boundary layer, we have

$$\frac{1}{2} u_\delta^2 + \left(\frac{p}{\rho} + gy\right)_\delta = \frac{1}{2} U_\infty^2 \tag{50}$$

Substitution of this in equation (48) gives

$$\left(\frac{p_o}{\rho} + g\zeta\right) = \frac{1}{2}\left(U_\infty^2 - u_\delta^2\right) - \int_0^\delta \kappa u^2 dn \tag{51}$$

and from equation (49)

$$\frac{\partial}{\partial s}\left(\frac{p}{\rho} + gy\right) = - u_\delta u_\delta' - \frac{\partial}{\partial s}\left\{\int_n^\delta \kappa u^2 dn\right\} \tag{52}$$

Also, integration of the continuity equation (37) gives

$$v = - \int_0^n \frac{\partial u}{\partial s}\, dn \tag{53}$$

Using equations (52) and (53), together with the boundary conditions of equations (10) and (41) in the viscous term, equation (38) can be integrated across the boundary layer from $n = 0$ to $n = \delta$. After some rearrangement this yields the momentum-integral equation in the form

$$\frac{d}{ds}\int_0^\delta u(u - u_\delta)dn + u_\delta' \int_0^\delta (u - u_\delta)\, dn$$
$$- \int_0^\delta \kappa u \frac{\partial}{\partial s} \int_0^n u dn dn - \frac{d}{ds}\int_0^\delta \int_n^\delta \kappa u^2 dn dn + \nu\kappa(u_o + u_\delta) = 0 \tag{54}$$

If the integrals in the above are evaluated using the velocity profile of equation (42), and terms of $O(\kappa\delta)^3$ are neglected, we obtain the rather simple momentum integral equation

$$\frac{d}{ds}\left\{\left(\frac{\alpha}{6} + \frac{1}{2}\right) u_o^3 \kappa \delta^2\right\} = 2\nu\kappa u_o^2 \tag{55}$$

so that

$$\delta^2 = \frac{12\nu}{(3 + \alpha)u_o^3 \kappa} \int_{-\infty}^s \kappa u_o^2 ds \tag{56}$$

Since $\alpha$ is given by equation (45), the above equation relates the boundary-layer thickness to the free-surface velocity, $u_o$, and shape, $\zeta$ and $\kappa$.

Another equation containing the above variables can be obtained from the normal-momentum equation (51) by substituting into it the velocity-profile relations (42) and (46), and using equations (44) and (45). This leads to

$$\delta \frac{d}{ds} \{\frac{1}{3} (4 + \alpha) u_o^2 \kappa\delta\} = - 2\nu\kappa\alpha u_o \tag{57}$$

Thus, equations (56) and (57) can be solved for $\delta$ and $u_o$ if the shape of the free surface (i.e., $\zeta$ and $\kappa$) is prescribed. Note that surface tension is involved through the parameter $\alpha$, and separation would be indicated by $u_o = 0$.

It is also of interest to evaluate the displacement and momentum thicknesses of the boundary layer. If the flow were potential, the velocity would vary according to equation (40) with $\omega = 0$. This gives the potential-flow velocity ($u_p$) distribution

$$u_p = u_\delta\{1+\kappa(\delta-n)\} \tag{58}$$

The integral thicknesses defined by

$$\delta^* = \frac{1}{u_\delta} \int_o^\delta (u_p - u)dn \tag{59}$$

and

$$\theta = \frac{1}{u_\delta^2} \int_o^\delta u(u_p - u)dn \tag{60}$$

can then be evaluated using equations (42), (46) and (58) to obtain

$$\kappa\delta^* = \frac{1}{6} (3 + \alpha) (\kappa\delta)^2 + O(\kappa\delta)^3 \tag{61}$$

and

$$\kappa\theta = \frac{1}{6} (3 + \alpha) (\kappa\delta)^2 + O(\kappa\delta)^3 \tag{62}$$

If equation (62) is combined with equation (56), we obtain the rather simple result

$$\theta = \frac{2\nu}{u_o^3} \int_{-\infty}^{s} \kappa u_o^2 ds \tag{63}$$

Since equation (63) does not contain the parameter $\alpha$, it can be readily integrated with the condition $\theta = 0$ at $s = -\infty$, provided $\kappa$ and $u_o$ are known,

to obtain an estimate of the momentum thickness. As a first approximation, we use the inviscid, irrotational-flow analysis of Section III, i.e., equation (23) to determine $\kappa$ and equation (24) to obtain $u_0$ (= U at y = 0). Figure 6 shows the development of the momentum thickness at Re = 2 x $10^5$ for several Froude numbers. It is seen that $\theta/a$ is of the order of $10^{-5}$ for distances of the order of one diameter upstream of the cylinder. The rapid growth of $\theta$ ahead of the obstacle also indicates the increased proneness to separation.

## V. CONCLUDING REMARKS

The flow ahead of a semi-submerged two-dimensional body moving through a viscous liquid is considered. Examination of the exact boundary conditions at the free surface has shown that surface tension plays a critical role in the determination of the free-surface velocity. The simplifying assumption of no pressure jump across the free surface then leads to the prediction of a stagnation point ahead of the body. This, in turn, explains the origin of vortices ahead of the body which have been observed in experiments. the predictions of the simple theory are in qualitative agreement with experimental results. Possible reasons for some discrepancies in the available experimental data, and the lack of more precise agreement with the theory, have been suggested.

A detailed analysis of the equations of motion has been carried out to derive the equations of the free-surface boundary layer which contains the vorticity generated by the surface curvature. An integral method has been utilized to obtain two ordinary differential equations which relate the boundary-layer thickness and free-surface velocity to the curvature and slope of the free surface. These remove the restrictive assumption on the pressure jump and should lead to a more accurate prediction of the separation and vortex location. Solutions of these equations are in progress.

Finally, we note that the analysis presented here is restricted to a two-dimensional flow. Nevertheless, it provides an explanation for the existence of vortices observed ahead of ship models. Also, it can be generalized for application to three-dimensional flows and, in combination with the kinematic

theories of vorticity amplification (Hawthorne, 1954; Lighthill, 1956), as suggested by Mori (1984) and Takekuma and Eggers (1984), may lead to a rational theory for the prediction of the necklace vortices ahead of ships. The complex interaction between the free-surface boundary layer, the bow vortices and the overall flow pattern around the bow is a subject for further research, as is the connection between the bow vortices and the breaking of bow waves.

## REFERENCES

Batchelor, G.K. (1970), "An Introduction to Fluid Dynamics", Cambridge University Press.

Hawthorne, W.R. (1954), "The Secondary Flow about Struts and Airfoils", J. Aeron. Sci., Vol. 21, pp. 588-608.

Honji, H. (1976), "Observation of a Vortex in Front of a Half-Submerged Circular Cylinder", J. Physical Society, Japan, Vol. 40, No. 5.

Kayo, Y. and Takekuma, K. (1981), "On the Free-Surface Shear Flow Related to Bow Wave Breaking of Full Ship Models", J. Society Nav. Arch. Japan, Vol. 149.

Kayo, Y., Takekuma, K., Eggers, K. and Sharma, S.D. (1982), "Observations of Free-Surface Shear Flow and its Relation to Bow Wave-Breaking on Full Forms", Inst. Shiffbau, Univ. Hamburg, Rept. 420.

Landweber, L. and Patel, V.C. (1979), "Ship Boundary Layers", Ann. Rev. Fluid Mech., Vol. 11, pp. 173-205.

Lighthill, M.J. (1956), "Drift", J. Fluid Mech., Vol. 1, pp. 31-53.

Longuet-Higgins, M.S. (1953), "Mass Transport in Water Waves", Phil. Trans., Vol. A245, pp. 535-581.

Longuet-Higgins, M.S. (1960), "Mass Transport in the Boundary Layer at a Free Oscillating Surface", J. Fluid Mech., Vol. 8, pp. 293-306.

Maruo, H. (1983), Private communication.

Mori, K. (1984), "Necklace Vortex and Bow Wave Around Blunt Bodies", Proc. 15th ONR Symposium on Naval Hydrodynamics, 2-7 Sept., Hamburg.

Takekuma, K. and Eggers, K. (1984), "Effect of Bow Shapes on the Free-Surface Shear Flow", Proc. 15th ONR Symposium on Naval Hydrodynamics, 2-7 Sept., Hamburg.

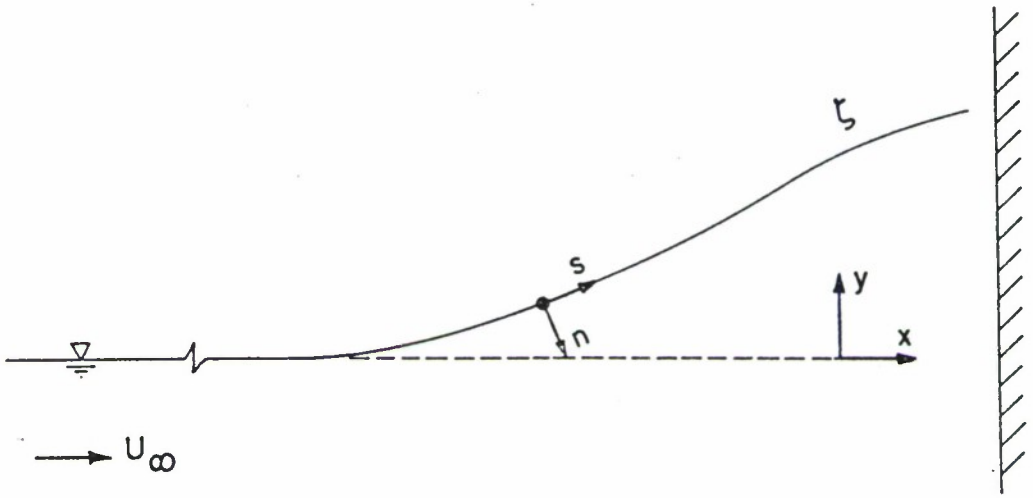


FIGURE 1. NOTATION

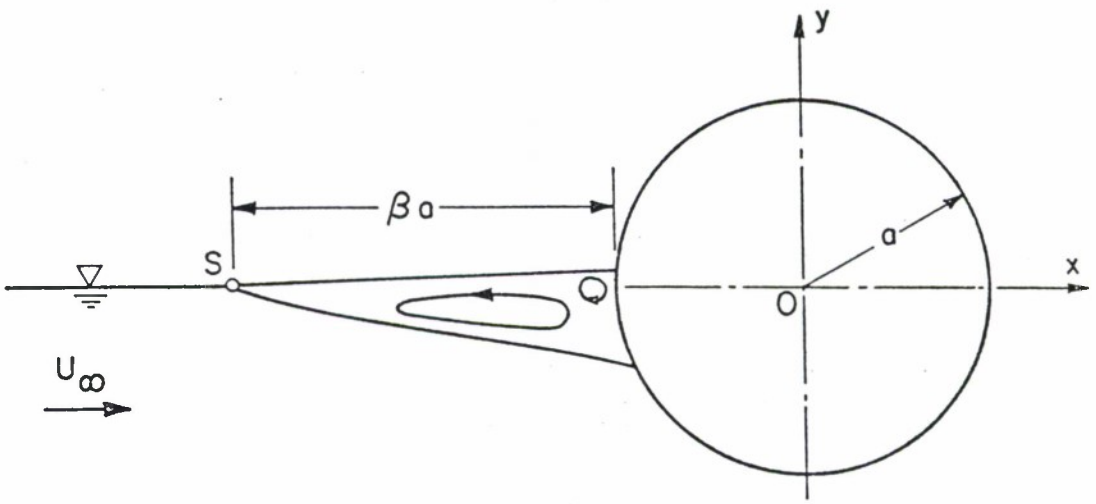


FIGURE 2. VORTICES AHEAD OF A TWO-DIMENSIONAL CYLINDER

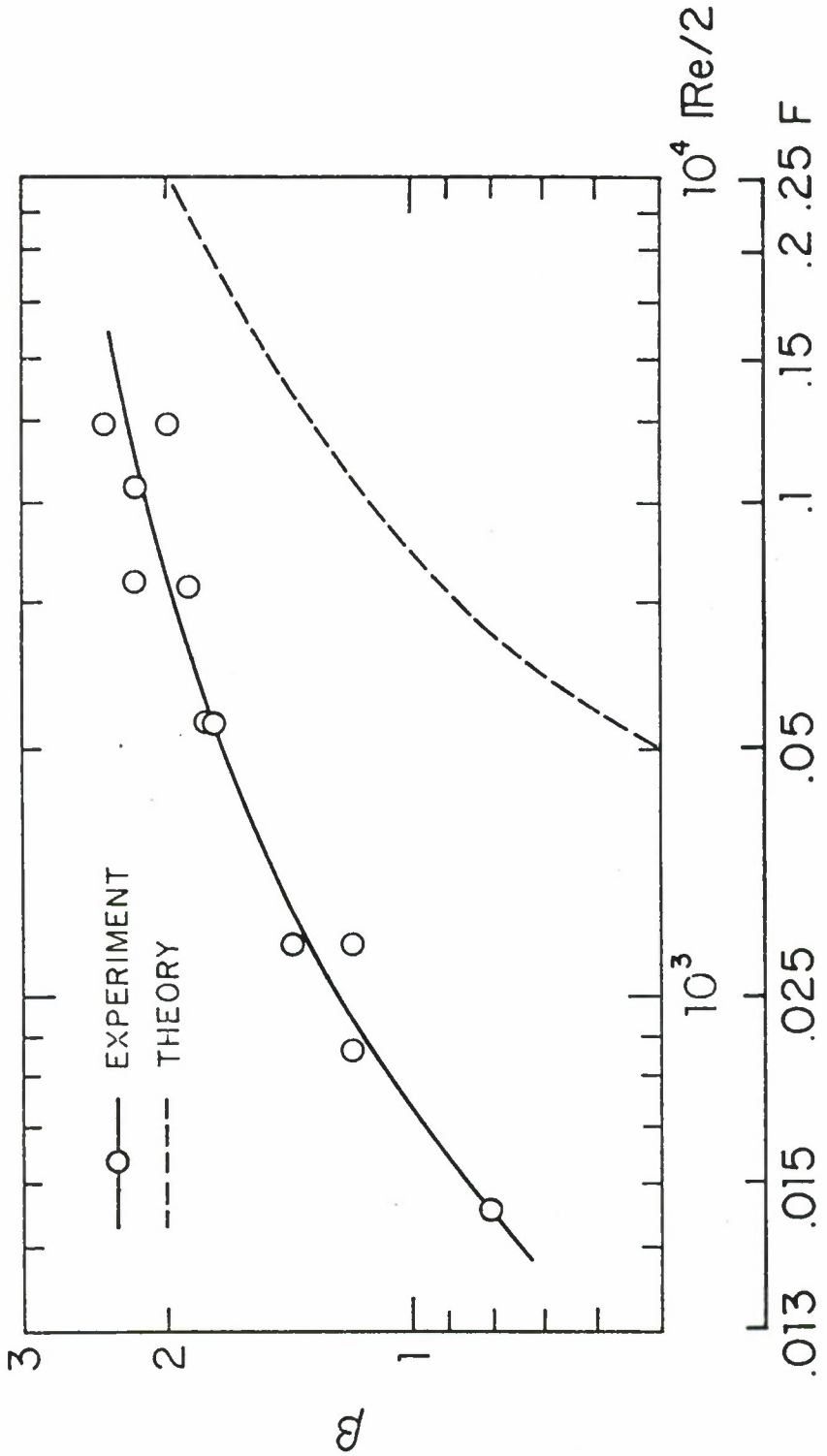


FIGURE 3. EXPERIMENTS OF HONJI (1976)

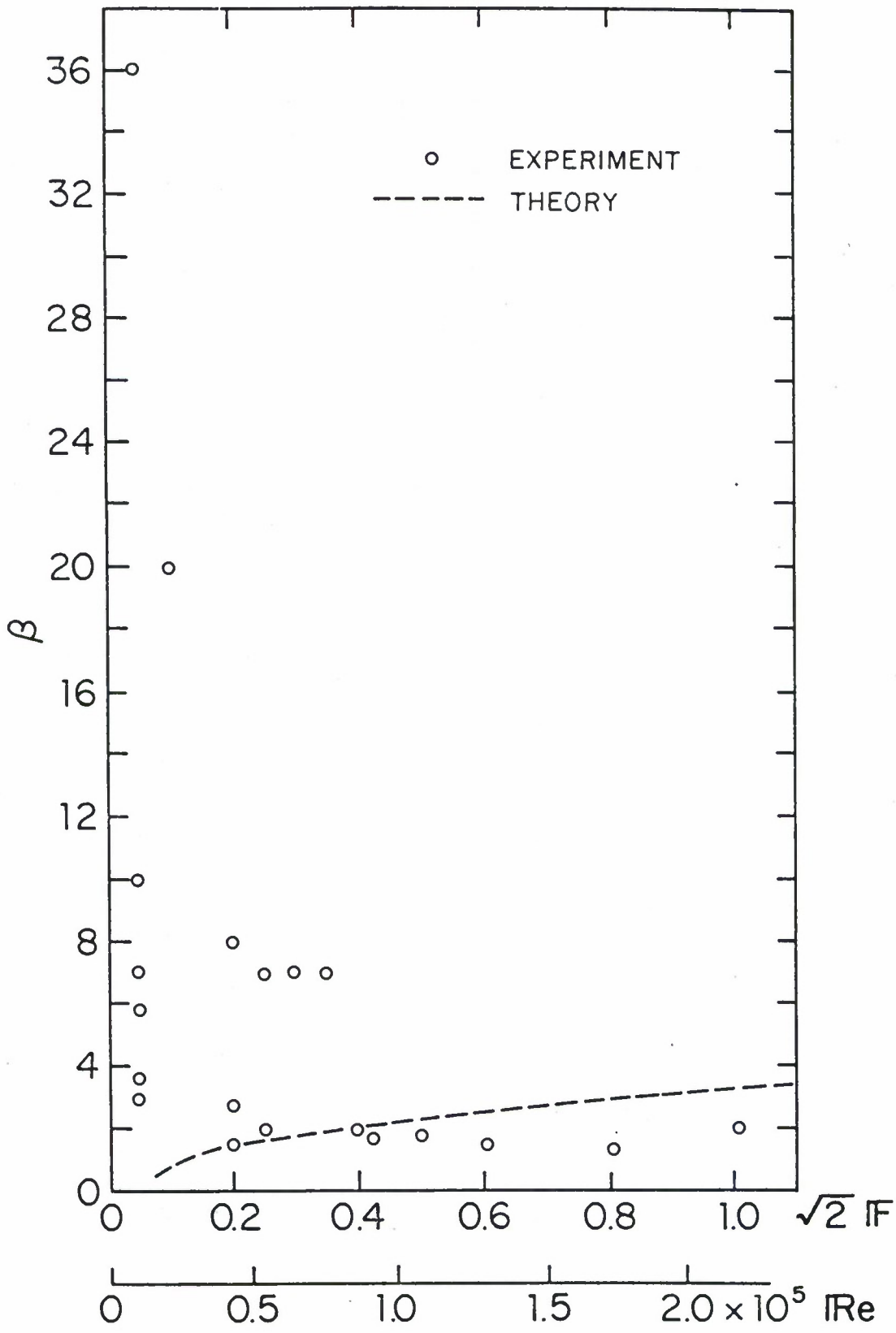


FIGURE 4. EXPERIMENTS OF KAYO ET AL. (1982)

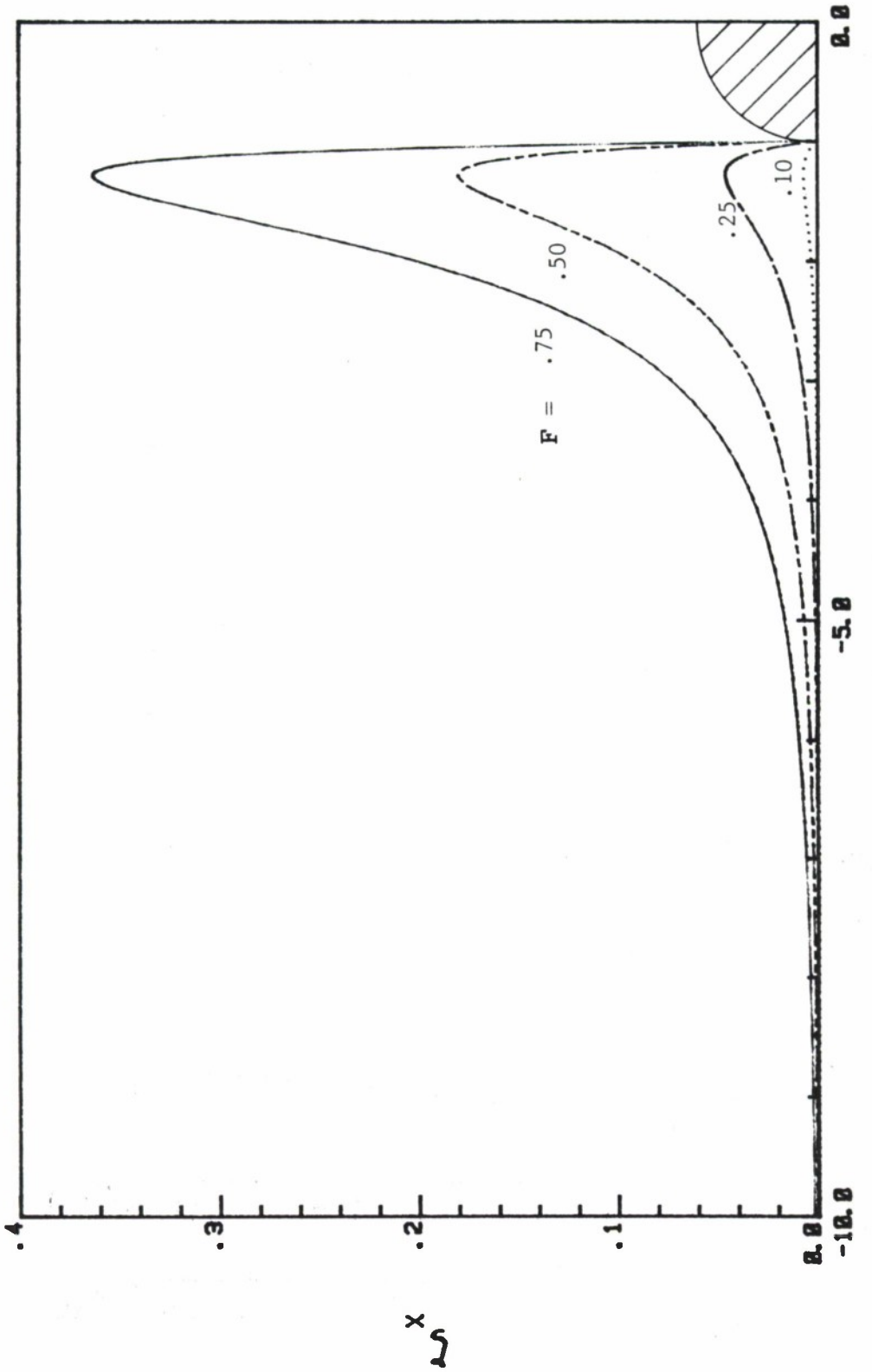


FIGURE 5. FREE-SURFACE SLOPE AHEAD OF A CYLINDER

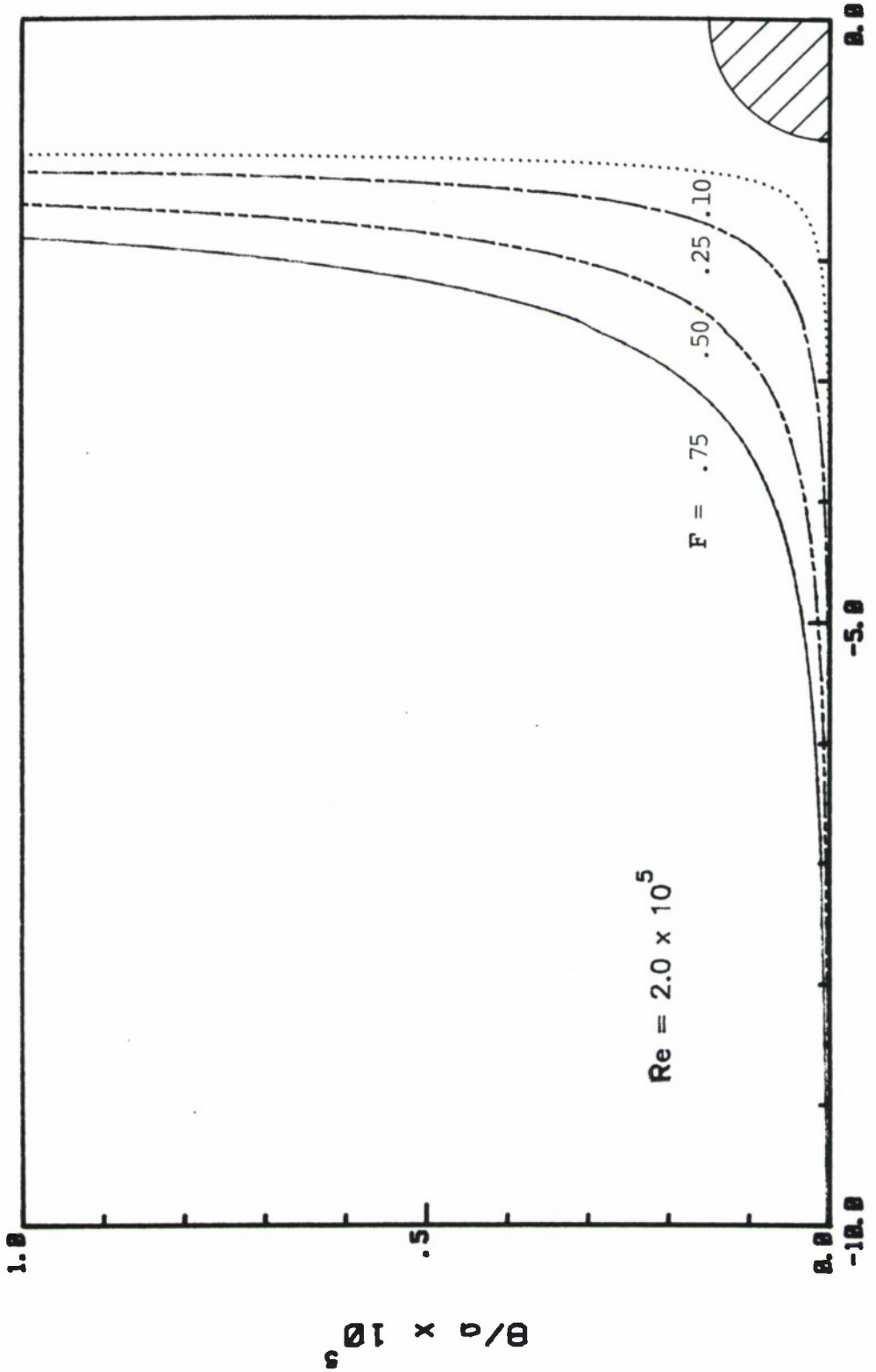


FIGURE 6. MOMENTUM THICKNESS OF THE FREE-SURFACE BOUNDARY LAYER AHEAD OF THE CYLINDER

# DISTRIBUTION LIST

Commander
David W. Taylor Naval Ship
R & D Center (ATTN: Code 1505)
Bldg. 19, Room 129B
Bethesda, Maryland 20084
15 Copies

Commander
Naval Sea Systems Command
Washington, D.C. 20362
ATTN: 05R22 (J. Sejd)

Commander
Naval Sea Systems Command
Washington, D.C. 20362
ATTN:55W (R. Keane, Jr.)

Commander
Naval Sea Systems Command
Washington, D.C. 20362
ATTN: 55W3 (W. Sandberg)

Commander
Naval Sea Systems Command
Washington, D.C. 20362
ATTN: 50151 (C. Kennell)

Commander
Naval Sea Systems Command
Washington, D.C. 20362
ATTN: 56X1 (F. Welling)

Commander
Naval Sea Systems Command
Washington, D.C. 20362
ATTN: 63R31 (T. Pierce)

Commander
Naval Sea Systems Command
Washington, D.C. 20362
ATTN: 55X42 (A. Paladino)

Commander
Naval Sea Systems Command
Washington, D.C. 20362
ATTN: 99612 (Library)

Director
Defense Documentation Center
5010 Duke Street
Alexandria, Va 22314
12 copies

Library of Congress
Science & Technology Division
Washington, D.C. 20540

Naval Ship Engineering Center
Norfolk Division
Combatant Craft Engr Dept
Attn: D. Blount (6660)
Norfolk, VA 23511

Naval Underwater Weapons Research
& Engineering Station (Library)
Newport, R.I. 02840

Office of Naval Research
800 N. Quincy Street
Arlington, Virginia 22217
ATTN: Dr. C.M. Lee, Code 432

Commanding Officer (L31)
Naval Civil Engineering Laboratory
Port Hueneme, CA 93043

Commander
Naval Ocean Systems Center
San Diego, CA 92152
Attn: Library

Library
Naval Underwater Systems Center
Newport, RI 02840

Research Center Library
Waterways Experiment Station
Corps of Engineers
P.O. Box 631
Vicksburg, Mississippi 39180

Charleston Naval Shipyard
Technical Library
Naval Base
Charleston, S.C. 29408

Norfolk Naval Shipyard
Technical Library
Portsmoth, VA 23709

Puget Sound Naval Shipyard
Engineering Library
Bremerton, WA 98314

Long Beach Naval Shipyard
Technical Library (246L)
Long Beach, CA 90801

Mare Island Naval Shipyard
Shipyard Technical Library (202.3)
Vallejo, CA 94592

Assistant Chief Design Engineer
for Naval Architecture (Code 250)
Mare Island Naval Shipyward
Vallejo, CA 94592

U.S. Naval Academy
Annapolis, Md 21402
Attn: Technical Library

Naval Postgraduate School
Monterey, CA 93940
Attn: Library (2124)

Study Center
National Maritime Research Center
U.S. Merchant Marine Academy
Kings Point, LI, New York 11024

The Pennsylvania State University
Applied Research Laboratory (Library)
P.O. Box 30
State College, PA 16801

Dr. B. Parkin, Director
Garfield Thomas Water Tunnel
Appliled Research Laboratory
P.O. Box 30
State College, PA

Bolt, Beranek & Newman (Library)
50 Moulton Street
Cambridge, MA 02138

Bethlehem Steel Corporation
25 Broadway
New York, New York 10004
Attn: Library-Shipbuilding

Cambridge Acoustical Associates, Inc.
54 Rindge Ave Extension
Cambridge, MA 02140

R & D Manager
Electric Boat Division
General Dynamics Corporation
Groton, Conn 06340

Gibbs & Cox, Inc. (Tech Info Control)
21 West Street
New York, New York 10006

Hydronautics, Inc. (Library)
Pindell School Rd.
Laurel, MD 20810

Newport News Shipbuilding and Dry
Dock Company (Tech. Library)
4101 Washington Ave.
Newport News, VA 23607

Mr. S. Spangler
Nielsen Engineering & Research, Inc.
510 Clyde Ave.
Mountain View, CA 94043

Society of Naval Architects and
Marine Engineers (Tech Library)
One World Trade Center, Suite 1369
New York, NY 10048

Sun Shipbuilding & Dry Dock Co.
Attn: Chief Naval A rchitect
Chester, PA 19000

Sperry Systems Management Division
Sperry Rand Corporation (Library)
Great Neck, N.Y. 10020

Stanford Research Institute
Attn: Library
Menlo Park, CA 94025

Southwest Research Institute
P.O. Drawer 28510
San Antonio, TX 78284
Attn: Applied Mech. Review
Dr. H. Abramson
2 copies

Tracor, Inc.
6500 Tracor Lane
Austin, Texas 78721

Mr. Robert Taggart
9411 Lee Highway, Suite P
Fairfax, VA 22031

Ocean Engr Department
Woods Hole Oceanographic Inc.
Woods Hole, Mass. 02543

Worcester Polytechnic Inst.
Alden Research Lab (Tech Library)
Worcester, MA 01609

Applied Physics Laboratory
University of Washington (Tech Library)
1013 N. E. 40th Street
Seattle, Washington 98105

University of California
Naval Architecture Department
Berkeley, CA 94720
4 Copies - ATTN: Profs. Webster, Paulling,
Wehausen & Library

California Institute of Technology
ATTN: Library
Pasadena, CA 91109

Engineering Research Center
Reading Room
Colorado State University
Foothills Campus
Fort Collins, Colorado 80521

Florida Atlantic University
Ocean Engineering Department
Boca Raton, Florida 33432
Attn: Technical Library

Gordon McKay Library
Harvard University
Pierce Hall
Cambridge, MA 02138

Department of Ocean Engineering
University of Hawaii (Library)
2565 The Mall
Honolulu, Hawaii 96822

Institute of Hydraulic Research
The University of Iowa
Iowa City, Iowa 52242
3 copies ATTN: Library, Landweber, Patel

Prof. O. Phillips
Mechanics Department
The John Hopkins University
Baltimore, Maryland 21218

Kansas State University
Engineering Experiment Station
Seaton Hall
Manhattan, Kansas 66502

University of Kansas
Chairman, Civil Engr Department Library
Lawrence, Kansas 60644

Fritz Engr Laboratory Library
Department of Civil Engr
Lehigh University
Bethelehem, PA 18015

Department of Ocean Engineering
Massachusetts Institute of Technology
Cambridge, MA 02139
2 Copies: Attn: Profs. Leehey & Kerwin

Engineering Technical Reports
Room 10-500
Massachusetts Institute of Technology
Cambridge, MA 02139

St. Anthony Falls Hydraulic Laboratory
University of Minnesota
Mississippi River at 3rd Ave., S.E.
Minneapolis, Minnesota 55414
2 Copies: Attn: Dr. Austin & Library

Department of Naval Architecture
and Marine Engineering - North Campus
ATTN: Library
University of Michigan
Ann Arbor, Michigan 48109

Davidson Laboratory
Stevens Institute of Technology
711 Hudson Street
Hoboken, New Jersey 07030
Attn: Library

Applied Research Laboratory
University of Texas
P.O. Box 8029
Austin, Texas 78712

Stanford University
Stanford, California 94305
2 Copies:
Attn: Engineering Library, Dr. Street

Webb Institute of Naval Archtecture
Attn: Library
Crescent Beach Road
Glen Cove, L.I., New York 11542

National Science Foundation
Engineering Division Library
1800 G Street N.W.
Washington, D.C. 20550

Mr. John L. Hess
4338 Vista Street
Long Beach, CA 90803

Dr. Tuncer Cebeci
Mechanical Engineering Dept.
California State University
Long Beach, CA 90840

Science Applications, Inc.
134 Holiday Court, Suite 318
Annapolis, MD 21401